ARTICLE NO. 79-0146R

GAU-8 Projectile Afterbody Drag Reduction by Boattailing and Heated Gas Injection

Wladimiro Calarese*
Air Force Flight Dynamics Laboratory, Wright-Patterson Air Force Base, Ohio

An experimental investigation was performed on a GAU-8 projectile model in order to determine whether base injection of different gases at a temperature of up to 900°R, which simulates the effects of fumers, would produce a reduction in the afterbody drag. Wind tunnel tests were performed at Mach 3, using different boattail angles and two different gases—air and helium. Pressure data were taken together with schlieren photographs illustrating the flowfield. Results show that afterbody drag reduction of 30-40% is obtained by small gas injection. Afterbody boattail angles of 4-7 deg additionally reduce the afterbody drag by about 15%. Heating the injected gas to 700°R does not further reduce the afterbody drag, but increasing its temperature up to 900°R produces an afterbody drag reduction of approximately 15%. For the same mass injection rates, helium injection is more efficient than air.

Nomenclature

$C_{D_{AB}}$ = afterbody drag coefficient based on maximum cross-sectional area (does not include rifling ring)
C_p = pressure coefficient
D = diameter
FR = fineness ratio = L/D_M
I = mass flow parameter = $\dot{m}/\rho_\infty u_\infty S_M$
l = boattail axial length
L = model axial length
$\dot{m}$ = mass flow
p = pressure
S = cross-sectional area
T = temperature
T_0 = stagnation temperature
u = longitudinal velocity
x = coordinate in the longitudinal direction
β = boattail angle
ρ = density

Subscripts and Superscripts

b = base
g = gas
j = jet
M = maximum
∞ = freestream
β = boattail
$( )'$ = first derivative
$\bar{( )}$ = nondimensionalized with respect to l

Introduction

THE high afterbody drag penalties incurred in supersonic flow by slender bodies of revolution have stimulated many investigators to find some methods that might give a reduction in the afterbody drag. An attempt to reduce the afterbody drag of a GAU-8 30-mm projectile was first made by Freeman and Korkegi.[1] They used boattailing of the afterbody and base blowing of cold gases to reduce the projectile drag. Subsequently, Calarese and Walterick[2] performed an experimental investigation to optimize the results of Ref. 1 and used a combination of boattail and base injection of gases heated up to 700°R. This combination did not improve the results obtained with base injection alone. The present investigation treats the base injection problem with particular emphasis on the temperature of the injected gases, which now attain 900°R. The injection of hot gases was used to simulate fumer elements, i.e. elements that vaporize by reaction with given oxidizers and burn at given temperatures, such as those used in tracers. One of the two gases used, air, was selected to simulate the molecular weight of typical products of combustion, which is 20-25.

In order to find the optimum condition for minimum drag, a tradeoff between boattail and base drag must be used. Base pressure problems have been studied by many.[3] The base drag is generated by the low pressure created by the shear layer that separates at the base corner and usually undergoes a strong expansion. In order to increase the base pressure and reduce the drag, gas injection has been used in the past.[4-8] Many parameters contribute to the value of the afterbody drag, such as injection rate, boattail angle, injection temperature, type of gas or gas mixture, boundary-layer characteristics, Mach number, Reynolds number, etc. The effects of these parameters have been extensively analyzed.[2]

Equipment and Test Description

The experiment was performed at two different wind tunnels, the High Reynolds Number Facility[9] (HiReF) and the Trisonic Gasdynamic Facility[10] (TGF).

The Mach 3 wind tunnel of the HiReF is a two-dimensional cold flow blowdown type wind tunnel with an 8×8.2 in. test section. The tests were conducted on a full-size strut mounted projectile model (Figs. 1 and 2) illustrated in detail in Ref. 1, at Mach 2.93, a stagnation pressure of 75 psia and a Reynolds number of 8×10^6 based on the model length. The projectile fineness ratio is 5.15. Base injection of air and helium was used.

The TGF consists of a closed-circuit two-dimensional wind tunnel for subsonic, transonic, and supersonic flow. The size of the test section is 23.7×23.7 in. The tests were conducted at Mach 3, a tunnel stagnation pressure of 24.3 psia, a stagnation temperature of 550°R, and a Reynolds number of 4.8×10^6 and 5.3×10^6 based on the model lengths. The

Presented as Paper 79-0146 at the 17th Aerospace Sciences Meeting, New Orleans, La., Jan. 15-17, 1979; submitted Feb. 12, 1979; revision received June 11, 1979.

Index categories: Jets, Wakes, and Viscid-Inviscid Flow Interactions; Supersonic and Hypersonic Flow.

*Aerospace Engineer.

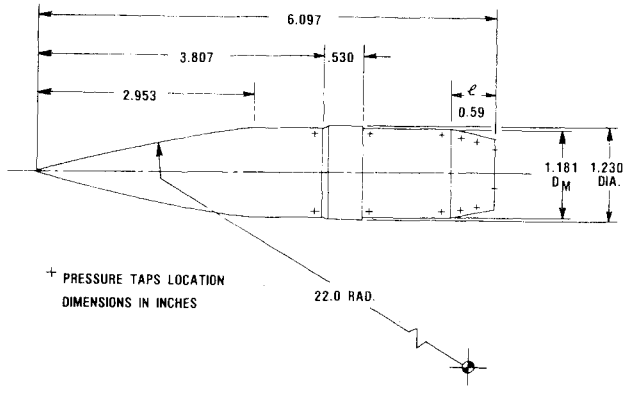

Fig. 1 Full-scale drawing, 5.15 fineness ratio used in the HiReF.

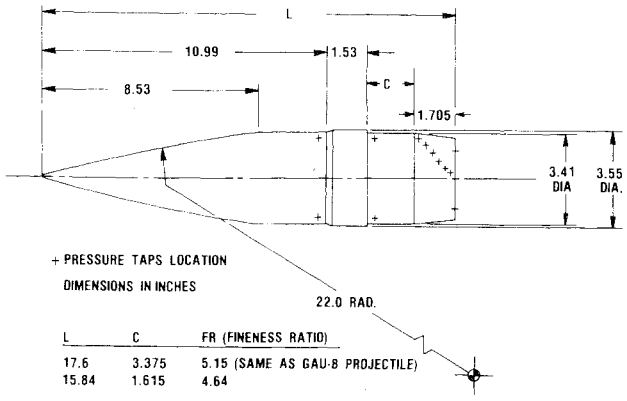

Fig. 3 2.8 times scale drawing, 4.64 fineness ratio used in the TGF.

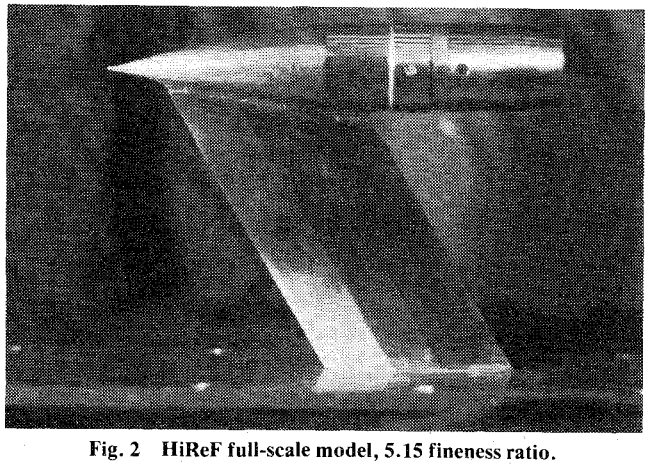

Fig. 2 HiReF full-scale model, 5.15 fineness ratio.

model is approximately a 2.8 times scale version of a GAU-8 30-mm projectile. It is strut mounted with a maximum diameter of 3.41 in. (excluding the rifling ring), two different overall lengths, one of 17.60 in., and the other of 15.84 in. in order to obtain two fineness ratios, one the same as the projectile, 5.15, and the other 4.64, to alter the turbulent boundary-layer characteristics without appreciably affecting the external flow (Fig. 3). In Ref. 2 two models were tested, the full-scale model of 5.15 fineness ratio with cold injection, and the 2.8 times scale model of 4.64 fineness ratio with gas injection of 520°R and 700°R temperature. In the present study the 2.8 times scale model of 4.64 and 5.15 fineness ratio and the full-scale model of 5.15 fineness ratio have been tested with cold and hot gas injection up to 900°R temperature.

The strut's sweepback angle was 60 deg, the leading and trailing half-angles 8.64 deg each, and the maximum thickness 0.25 in. for the HiReF model and 0.72 in. for the TGF model. A strut of this type has little effect on the base pressure.[11] No strut effects were noticed in the pressure data and schlieren photographs of this experiment.

Afterbodies of different boattail angles were tested, however, the emphasis was placed on $\beta = 4$-7 deg due to the results presented in Ref. 2. The shape and the caliber of the boattails were selected after consultation with the AF Armament Laboratory. The conical ½ caliber boattails were selected due to stability and projectile fabrication requirements. The models were equipped with 10 to 13 static pressure taps, one or two ahead and behind the rifling ring located in the 0-deg meridian plane of the model and 180 deg apart; 4 to 6 pressure taps were located on the boattails 15 deg apart from each other peripherally; and 2 to 3 pressure taps were located in the base area, flush with the model in the 0-180-deg meridian plane (see Figs. 1 and 3). The average of the base pressure readings was used, since in most cases the readings were virtually identical. In addition two high-response transducers were also used in the TGF to measure dynamic pressures, one on the boattail and the other in the base region. They were referenced to a variable pressure system which was manually set and recorded for each test point. Voltage readouts from the transducers were fed directly to the TGF minicomputer where dynamic pressure coefficients were calculated. The model pressure transducers were connected to the computer for the calculation of the afterbody pressure drag. A thermocouple was installed inside the model settling chamber to measure the temperature of the injected gas. The maximum injection temperature attained was 1100°R in the HiReF and 900°R in the TGF.

The bases consisted of 5-6 μ porous metal disks used for base injection with injection diameters of 1.44, 1.75, and 1.8 in. for the TGF model which correspond to an injection diameter to maximum diameter ratio of $D_j/D_M = 0.42$, 0.51, and 0.52, respectively, and 0.62-in. diameter for the HiReF model, which corresponds to $D_j/D_M = 0.52$.

The mass flow system provided the secondary flow for cold and hot gas injection. The secondary flow was measured using a choked orifice. The mass flow parameter I used in the present study is the ratio of the mass flow injected and the mass flow captured by a stream tube of area equal to the model's maximum cross-sectional area S_M, which does not include the rifling ring.

Experimental data were obtained in both the HiReF and the TGF. In this manner, full-scale and 2.8 times scale results could be compared. The same proportions between tunnel size and model size were maintained in both facilities to ascertain if different wind tunnels would affect the results. The afterbody drag values obtained were plotted vs the mass flow parameter I and the boattail angle β.

The flowfield over the projectile afterbody can be seen in the schlieren photographs of Figs. 4 and 5. It can be observed that the increase in base injection rates changes considerably the near wake and produces an opening in the wake throat. The expansion at the base corner decreases, the strength of the shock at the wake throat also decreases, and the base pressure becomes higher. Further increases in injection rates eliminate the shock at the wake throat and produce a shock at the base corner, signifying that the base pressure has become higher than the boattail pressure. The corner shock losses are more than offset by the base pressure rise. Additional increases in injection rates add momentum to the wake and the entrainment action begins causing an early closure of the near wake and a base pressure decrease. Previous investigators[5] have found that this reversal in base pressure occurs simultaneously with the injection becoming supersonic. It is likely that the supersonic injection produces the strong entrainment action. The afterbody drag decreases at first for small injection rates but reverses its trend and increases for higher injection rates.

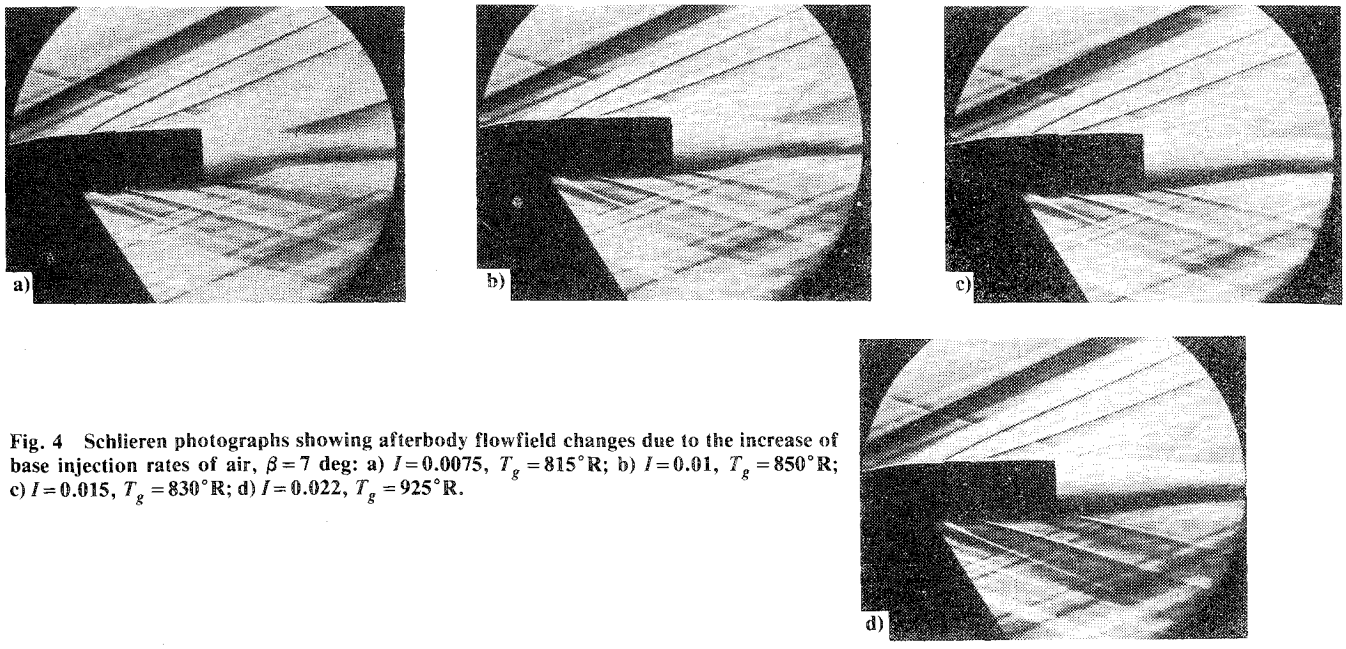

Fig. 4 Schlieren photographs showing afterbody flowfield changes due to the increase of base injection rates of air, $\beta = 7$ deg: a) $I = 0.0075$, $T_g = 815°R$; b) $I = 0.01$, $T_g = 850°R$; c) $I = 0.015$, $T_g = 830°R$; d) $I = 0.022$, $T_g = 925°R$.

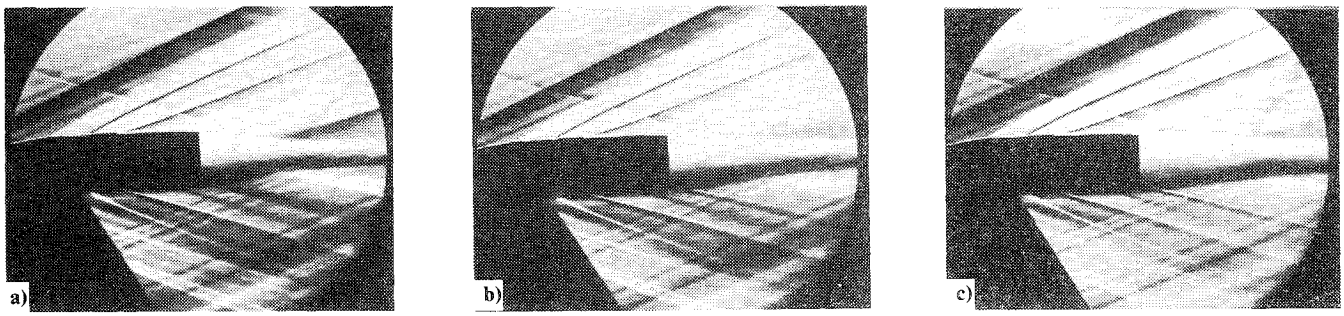

Fig. 5 Schlieren photographs showing afterbody flowfield changes due to the increase of base injection rates of helium, $\beta = 7$ deg: a) $I = 0.0036$, $T_g = 830°R$; b) $I = 0.00475$, $T_g = 900°R$; c) $I = 0.006$, $T_g = 905°R$.

The afterbody drag was calculated as follows:

$$C_{D_{AB}} = \frac{I}{S_M}\int_0^I C_{p_\beta} S' \mathrm{d}x - C_{p_b}\frac{S_b}{S_M} \tag{1}$$

which becomes

$$C_{D_{AB}} = \frac{8}{\bar{D}_M^2}\tan^2\beta\int_0^I C_{p_\beta}\bar{x}\mathrm{d}\bar{x} - \frac{4}{\bar{D}_M}\tan\beta\int_0^I C_{p_\beta}\mathrm{d}\bar{x} - C_{p_b}\left(I - \frac{2}{\bar{D}_M}\tan\beta\right)^2 \tag{2}$$

and for $\beta = 0$ deg

$$C_{D_{AB}} = -C_{p_b} \tag{3}$$

Some difficulties were encountered during the tests in the HiReF (blowdown type) with regard to pressure values obtained at low injection rates and high temperatures. At low injection rates, the temperature drop of the injected gas was very rapid. Starting with a gas temperature of 1000°R, by the time the readings were taken after the transient period, the temperature was too low (about 750°R) to be of any significance. To have an idea of how much the temperature values would affect the base pressure, it is useful to show a correlation[6] of base pressure changes with temperature increases of the injected gas

$$p_{\text{base}}/p_\infty = (p_{\text{base}}/p_\infty)_{I=0} + (12.25 + 0.002778\Delta T)I \tag{4}$$

where $\Delta T = T_g - T_{0_\infty}$. If ΔT is of the order of 200°R, the change in afterbody drag is only 1-2%, well within the experimental error. It is necessary therefore to increase the injected gas temperature to approximately 1000°R to obtain a sizeable change of about 8-10%. It was necessary then to heat the gas to be injected to a much higher than needed temperature, approximately 1200°R, to achieve injection temperatures of at least 900°R. Very careful monitoring of the heater was required to check for hot spots which might have burned it.

Another problem encountered was due to the long time it took for the pressure transducers to become stable after the tunnel start, so that the readings could be taken. This time lag, about 30 s, was due to the large pressure difference between tunnel atmospheric values at the start and low local pressure levels at $M_\infty \simeq 3$, and produced very high heat losses, lowering the injected gas temperature below 800°R. It was then decided to keep the pressure transducers closed for the first 10-15 s after the tunnel start (at almost vacuum conditions) to let the flow settle and avoid the transient period. Then the lines were opened and the pressure taps reached a steady value immediately so that the readings could be taken at a higher temperature, at least $T_g = 900°R$.

No unsteady pressures were detected on the TGF models. The root-mean-square of the pressure fluctuations was obtained in the TGF using the high-response transducers located in the afterbody region. When divided by the freestream dynamic pressure, its value was of the order of 10^{-3} to 10^{-4}. For the TGF this is a very low value within the noise level, indicating the presence of steady flow conditions.

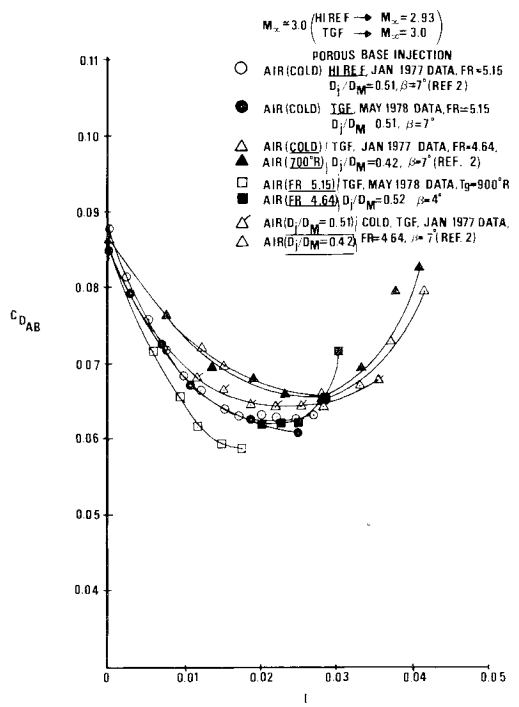

Fig. 6 Comparison of afterbody drag coefficients for different conditions.

Results

For the air injection case, the afterbody drag coefficient was plotted in Figs. 6 and 7 vs the mass-flow parameter. In Fig. 6 the present data are compared with previous data of Ref. 2 to ascertain whether different wind tunnels, model's fineness ratios, and injection diameters would affect the results. Small rates of mass injection through the base produce at first a drag coefficient reduction but the trend reverses itself with increasing injection rates. No appreciable tunnel effects are noticed. The increase of the temperature of the injected air from room tempreature (520°R) to 700°R did not produce any drag reduction in the experiment of Ref. 2. The difference in the model fineness ratio produced only a small change, about 5%, in the afterbody drag levels. The higher FR model, which represents a more slender body, yielded less drag. The effect of the injection diameter ratio is also shown in Fig. 6. The afterbody drag levels are about 5% lower for the higher injection diameter ratio. Figure 7 shows the effects produced by the injection in the base region of gases heated up to 900°R. For a given injection rate drag reduction increases with increasing temperature. The maximum drag reduction due to heat addition is of the order of 10-15%. The 5-deg angle boattail seems to be the most effective in drag reduction since it produces the same drag reduction as the 7-deg angle boattail, but at a lower injection rate.

The 900°R injection data from both tunnels are consistent. There are three basic drag levels, for any injection rate, observable in these figures: 1) high drag for low FR and small D_j, 2) lower drag for high FR and large D_j, and 3) lowest drag for high FR, large D_j, and heat addition.

Figure 8 shows the drag coefficient variation due to helium injection. The same trend as for air is seen, i.e. a considerable drag reduction due to small injection, a drag increase (reversal) at higher injection rates and for the same injection rate, lower drag for higher injection temperatures. One more feature is detected—the drag curves for cold helium injection are appreciably different for different fineness ratios, i.e. the lower drag curves are obtained for the higher FR (it is believed that this phenomenon is due not only to a better pressure recovery on the more slender body but also to a better mixing between the helium and the air flow).

Figure 9 compares the effects of air and helium on afterbody drag reduction. It is evident that hot helium injection gives a better drag reduction than cold helium injection and that, for the same mass injection rate, helium is more effective than air. If Figs. 4 and 5 are re-examined keeping in mind the effectiveness of the helium, it is easy to understand the difference in the shock pattern in the wake of the two gases. For mass injection rates of $I = 0.006$ for the helium and $I = 0.0075$ for air, close enough rates for comparison, it is observed that the base pressure with air injection is lower than the boattail pressure. An expansion then occurs at the boattail separation corner. The base pressure with helium injection is instead higher than the boattail pressure, since a quite strong shock emanates from the base separation corner. Since the boattail pressures are equal for both gases for lack of upstream influence, it is evident that helium injection pressurizes the base region more than air injection, which results in a better drag reduction. This helium effectiveness is attributed to its higher molecular weight which produces a higher speed of sound and

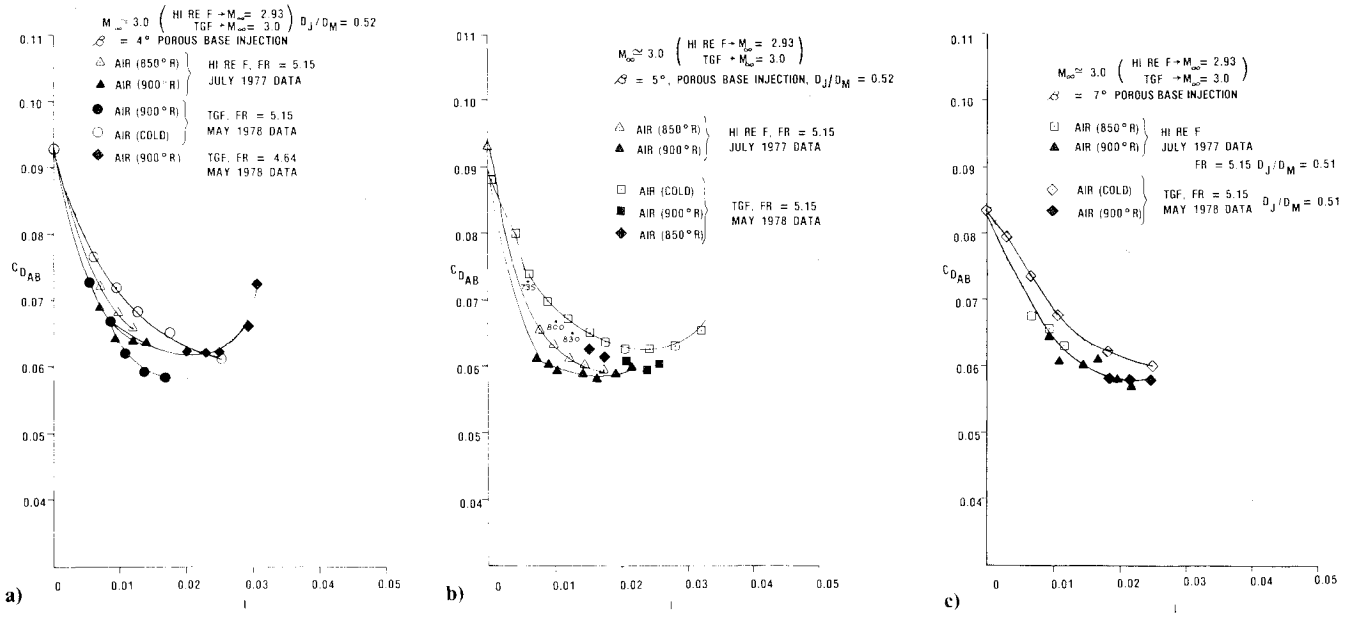

Fig. 7 Afterbody drag coefficient for air injection: a) $\beta = 4$ deg, b) $\beta = 5$ deg, c) $\beta = 7$ deg.

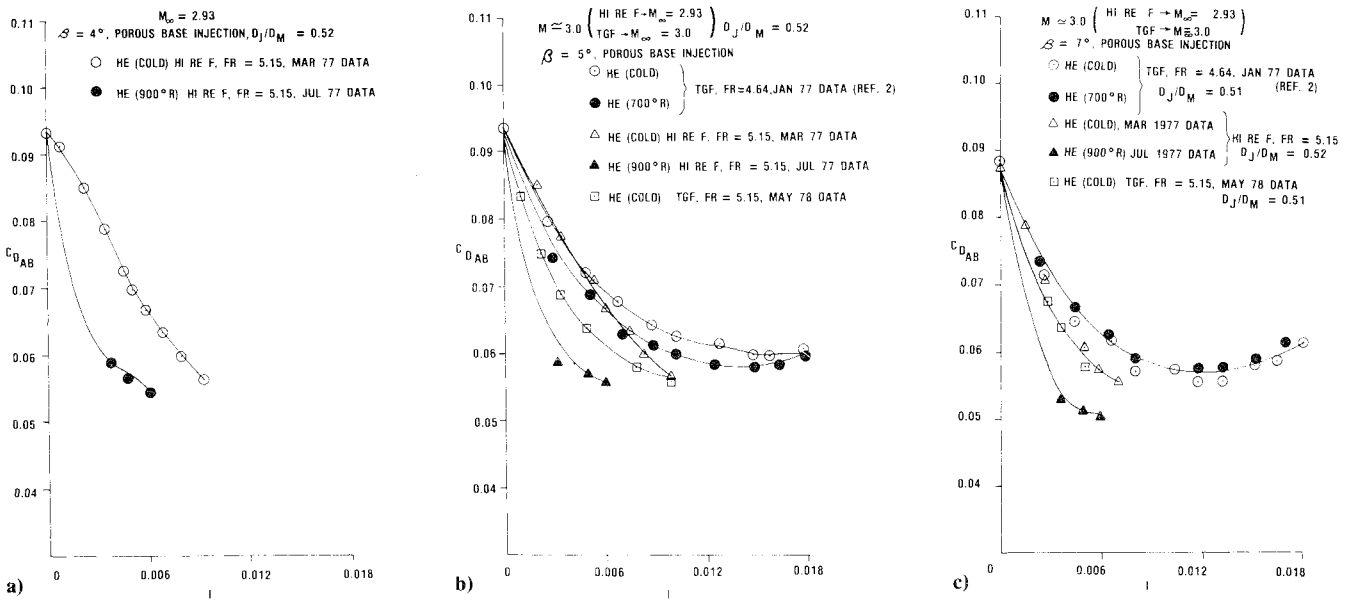

Fig. 8 Afterbody drag coefficient for helium injection: a) $\beta = 4$ deg, b) $\beta = 5$ deg, c) $\beta = 7$ deg.

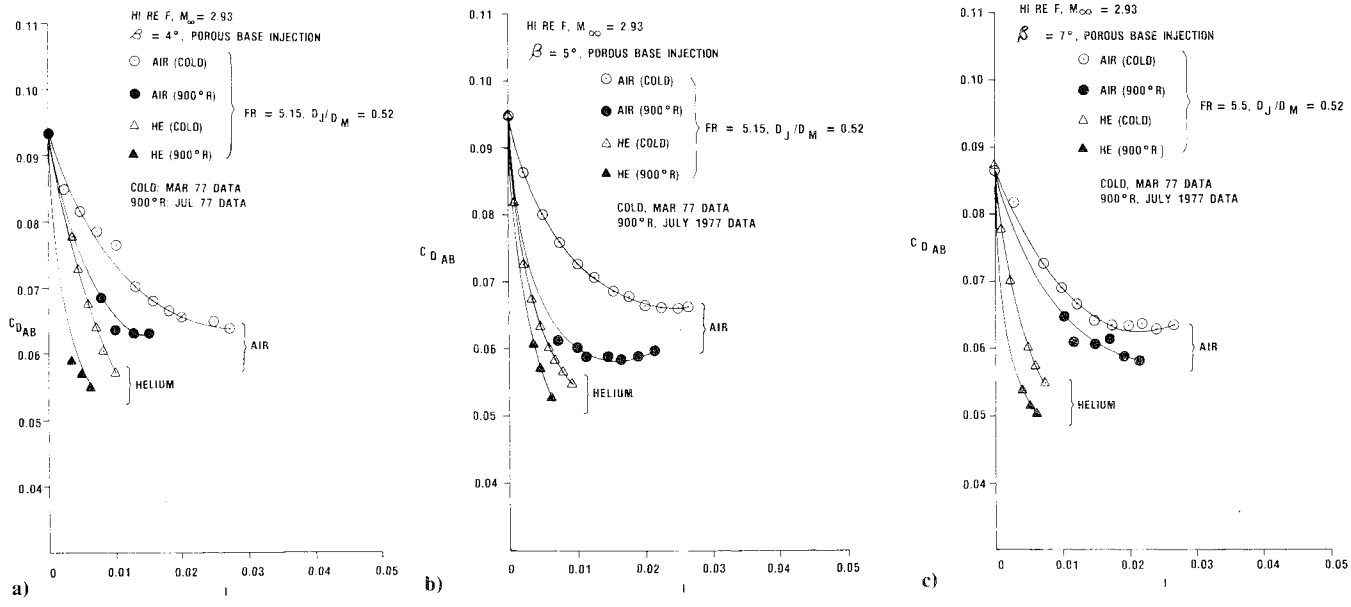

Fig. 9 Effects of air and helium injection on afterbody drag coefficient: a) $\beta = 4$ deg, b) $\beta = 5$ deg, c) $\beta = 7$ deg.

Fig. 10 Effect of boattail angle on afterbody drag coefficient with porous base injection: a) HiReF, $M_\infty = 2.93$; b) TFG, $M_\infty = 3.0$.

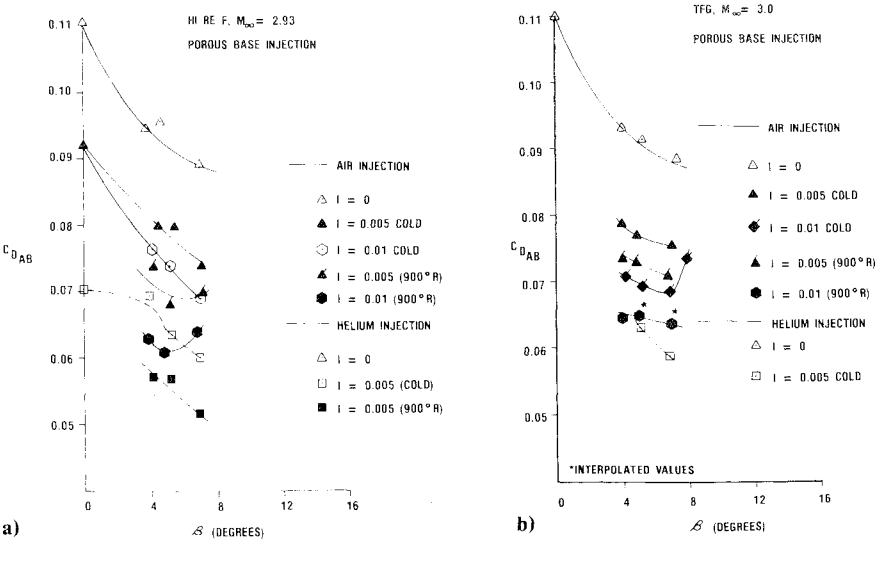

mass diffusion.[12] In addition, for a given injection rate the volumetric flow of helium is more than 3 times that of air. This higher volumetric flow contributes to the fast increase in the base pressure, since it increases the wake size decreasing the expansion at the base separation corner.

Figure 10 shows how the boattail angle affects the drag coefficient. At first the increase in β produces a drag reduction, but a further increase produces a reversal in the drag curves and a drag increase. This reversal is physically correct. For low boattail angles, as mentioned, the small expansion on the boattail shoulder which causes boattail drag is more than offset by the base pressure rise due to a lower expansion at the base separation corner so that the overall effect is an afterbody drag reduction. For higher angles the boattail drag becomes predominant and the total afterbody drag increases again. The boattail angle effect is similar to the mass injection effect. For injection rates up to $I=0.01$, the optimum condition seems to be at $\beta=7$ deg for air and helium injection with heat addition, with the exception of hot air injection in the HiReF for which the optimum condition is $\beta=5$ deg.

Conclusions

An experimental investigation ws performed on a GAU-8 projectile model at $M_\infty \simeq 3$ to obtain the best possible afterbody drag coefficient reduction by means of base injection with heat addition. Air and helium were used in the investigation. The hot injection tests were performed to simulate fumer elements. Through model modifications and improved testing techniques the injected gas temperature was increased to 900°R producing favorable results. It is possible that a further increase in temperature might produce a higher drag reduction. Additional tests are therefore recommended.

1) A reduction of the afterbody drag coefficient of up to 30% was obtained by small amounts of base injection of air and up to 40% when helium was used.

2) Afterbody boattail angles of 4-7 deg produced an additional drag reduction of about 15%. The 7-deg boattails appear to be more efficient.

3) Heating the injected gases to 700°R did not produce significant changes in the afterbody drag coefficient values, but increasing the temperature of the gases to 900°R produced a further afterbody drag reduction of about 15-20%.

4) For the same mass injection rates, helium injection was more efficient than air. (This result was attributed to the lighter molecular weight of the helium which increases the speed of sound through the gas, produces a better mass diffusion effect, and gives a volumetric flow which is approximately 3.5 times that of the air. A greater base pressure increase is therefore achieved and consequently a lower drag.)

5) The lower drag levels were obtained for the model with the higher fineness ratio, larger injection diameter, and by heating the injected gas to at least 900°R.

References

[1] Freeman, L.M. and Korkegi, R.H., "Projectile Aft-Body Drag Reduction by Combined Boat-Tailing and Base Blowing," AFAPL-TR-75-112, Feb. 1976.

[2] Calarese, W. and Walterick, R.E., "GAU-8 Projectile Afterbody Drag Reduction by Base and Boattail Injection," AFFDL TM-77-27-FXM, March 1977.

[3] Murthy, S.N.B. and Osborn, J.R., "Base Flow Data With and Without Injection: Bibliography and Semi-Rational Correlations," School of Mechanical Engineering, Purdue University, Contract No. DAAD 05-72-C-0342, (BRL), May 1973.

[4] Cortright, E.M., Jr. and Schroeder, A.H., "Preliminary Investigation of Effectiveness of Base Bleed in Reducing Drag of Blunt-Base Bodies in Supersonic Stream," NACA RM E51A26.

[5] Lewis, J.E. and Chapkis, R.L., "Mean Properties of the Turbulent Near Wake of a Slender Body With and Without Base Injection," *AIAA Journal,* Vol. 7, May 1969, pp. 835-841.

[6] Clayden, W.A. and Bowman, J.E., "Cylindrical Afterbodies at $M_\infty=2$ With Hot Gas Ejection," *AIAA Journal,* Vol. 6, Dec. 1968, pp. 2429-2431.

[7] Bowman, J.E. and Clayden, W.A., "Boat-Tailed Afterbodies at $M_\infty=2$ With Gas Ejection," *AIAA Journal,* Vol. 6, Oct. 1968, pp. 2029-2030.

[8] Bowman, J.E. and Clayden, W.A., "Reduction of Base Drag by Gas Ejection," Royal Armament Research and Development Establishment, Fort Halstead, Kent, U.K., R.A.R.D.E. Rept. 4/69, Dec. 1969.

[9] Fiore, A.W., Moore, D.G., Murray, D.H., and West, J.E., "Design and Calibration of the ARL Mach 3 High Reynolds Number Facility," ARL TR-0012, Jan. 1975.

[10] White, H.L., "Trisonic Gasdynamic Facility User Manual," AFFDL-TM-73-82-FXM, June 1973.

[11] Bowman, J.E. and Clayden, W.A., "Cylindrical Afterbodies in Supersonic Flow With Gas Ejection," *AIAA Journal,* Vol. 5, Aug. 1967, pp. 1524-1525.

[12] Fox, H., Zakkay, V., and Sinha, R., "A Review of Problems in the Nonreacting Turbulent Far Wake," *Astronautica Acta,* Vol. 14, 1968-69, pp. 215-228.